Gao et al. One Health Advances (2024) 2:24
https://doi.org/10.1186/s44280-024-00055-x

One Health Advances

ARTICLE

Open Access

Efficacy of Qi-Gen powder for immunity enhancement and investigation of its therapeutic mechanisms through gene expression profiling

Xueyan Gao[1,2†], Pingping Wang[1,2†], Shaolin Wang[1], Fenfang Yang[1,2], Danyang Ma[1,2], Xiaoqin Xu[3], Tingting Huang[1,2], Huisheng Xie[4*] and Zhihui Hao[1,2*]

Abstract

Infection with different viruses threatens the health of animals in the livestock and poultry industry. Immunopotentiators can increase natural immunity and vaccination efficacy; however, most are expensive chemical and biological compounds with questionable safety. Traditional Chinese medicines (TCMs) such as Yupingfeng (YPF), a well-known immunomodulatory remedy, provide healthy alternatives to such agents. The aim of this study was to examine the therapeutic properties of Qi-Gen powder (QG) and compare them with those of YPF. The immune organ index, cytokine levels, and other indicators were utilized to evaluate the effects of QG in an immunosuppression mouse model. QG was further assessed for its ability to enhance vaccine effectiveness in chickens immunized for Newcastle disease virus (NDV). Potential therapeutic mechanisms and targets of QG were examined in the breast cancer cell line MCF-7 using microarray technology combined with the TCM systems pharmacology database of known targets. Compared with model controls, QG improved immunological function, outperforming YPF in mice. QG also enhanced the immunological response to NDV vaccine in immune organs and increased feed intake of chickens. Further research is needed to validate the link between the PI3K/Akt/GSK-3 pathway and the immune-boosting effects of QG.

Keywords Traditional Chinese medicine, Immune function, Effect, Mechanism, Gene expression profiling analysis

Introduction

Humans and all other animals are susceptible to infectious diseases caused by viruses. During the last two decades, several viruses with substantial pathogenicity have had significant impacts, including severe acute respiratory syndrome coronavirus 2 [1], Middle East respiratory syndrome coronavirus [2], avian influenza virus [3], and classical swine fever virus [4]. The immune status of an organism has a significant impact on its capacity to recover from viral infectious illnesses, as demonstrated by the epidemiology of numerous historical outbreaks of viral infectious illnesses. Effective treatment and immune system boosting during viral infection require accurate diagnosis of the etiological agent.

†Xueyan Gao and Pingping Wang contributed equally to this work.

*Correspondence:
Huisheng Xie
shen@chiu.edu
Zhihui Hao
haozhihui@cau.edu.cn
[1] Chinese Veterinary Medicine Innovation Center, College of Veterinary Medicine, China Agricultural University, Beijing, China
[2] National Key Laboratory of Veterinary Public Health and Safety, College of Veterinary Medicine, China Agricultural University, Beijing, China
[3] Jiangsu Co-Innovation Center for Prevention and Control of Important Animal Infectious Diseases and Zoonoses, College of Veterinary Medicine, Yangzhou University, Yangzhou, China
[4] Chi University, 9650 W Hwy 318, Reddick, FL 32686, USA

Immunoenhancers can enhance the performance of natural immunity and vaccine-induced immunity. Although vaccines are an important way to prevent and treat viral infections, the majority of these biological and chemically created products are expensive to produce and come with safety concerns [5, 6].

Various traditional Chinese medicines (TCMs) have been demonstrated to promote the functions of immunological cells, immune organs, and cytokines, and to suppress the development of autoimmune, allergic, and inflammatory disorders [7]. Immunomodulatory TCMs have gained in popularity in recent years. For example, astragaloside IV has been used to treat inflammatory and immunological illnesses [8]; paeoniflorin, the major active component of *Paeonia lactiflora* Pallas, inhibits inflammation in animal models of autoimmune diseases, modulates immune cell functions and activation, decreases inflammatory medium production, balances the subsets of immune cells, and regulates certain signaling pathways [9]; Ginsenoside Re was used as an adjuvant to boost the immunological response to the inactivated rabies virus vaccine in mice [10]; and Jiedu Huayu granules have been shown to prevent liver damage by reducing inflammation through T-cell immunity [11]. Yupingfeng, also known as YPF, is another TCM that was originally used to treat respiratory conditions, but is now frequently clinically used as an anti-inflammatory and immunoregulatory medication [12]. In 2019, the Ministry of Agriculture and Rural Affairs of the People's Republic of China approved the use of the prescribed herbal medicine Qi-Gen powder (QG) in conjunction with a vaccine to boost immunity in chickens. YPF is a pure TCM preparation mainly comprising Huangqi, Baizhu, and Fangfeng. Huangqin (Scutellariae Radix, *Scutellaria baicalensis* Georgi, Labiatae) [13] and Banlangen (Isatidis Radix, *Isatis tinctoria* L., Cruciferae) are two conventional TCM remedies with immunoregulatory effects [14] that are combined with YPF to make QG. In this study, we investigated how the inclusion of Huangqin and Banlangen affected the prescription.

To assess the effects of QG on immune-mediated responses, two animal models were used in this study: mice with cyclophosphamide (CTX)-induced immunosuppression and Newcastle disease virus (NDV)-immunized chickens. CTX damages DNA structure and functionality, preventing DNA replication and protein synthesis, inhibiting cell division, and lowering immune function. To better understand the therapeutic mechanism and target of QG at the cellular level, we employed microarray technology, which is based on cellular gene expression, function, and response to the environment [15]. By comparing the expression profiles of various drugs, the potential mechanism and target of a medicine can be identified. Microarray technology is widely used in disease diagnosis [16] and drug discovery [17]. The Connectivity Map (cMap) tool integrates and analyzes pharmacogenomic data, revealing potential relationships between medications, genes, and diseases [18]. To investigate the mechanism of drug action of QG, we used cMap to create a massive library of distinct gene expression maps in the form of association diagrams. To further elucidate the mode of action of QG, a complex and multi-component medicine, we consulted the TCM Systems Pharmacology (TCMSP) database and analysis platform, which provides information on the intended uses and associated ailments of 499 Chinese herbal remedies listed in the Chinese Pharmacopoeia [19]. Finally, Gene Ontology (GO) annotation, Kyoto Encyclopedia of Genes and Genomes (KEGG) enrichment, and cMap analyses of the identified differentially expressed genes (DEGs) were integrated with known targets in the TCMSP database, revealing the pathway through which QG may regulate immune function.

Results

Effects of QG on immunologic function in immunosuppressed mice

To investigate the ability of QG to restore immune function in immunosuppressed mice, the CTX-induced model of immunosuppression was employed. Compared with the Control group, the model (CTX) group had significantly lower ($p < 0.05$ or $p < 0.01$) immune organ indexes (thymus and spleen), hemolysin antibody levels, and concanavalin A (Con A) stimulation index (Fig. 1). These results suggested that the modeling of immunosuppression was successful.

In comparisons between the TCM-treated groups and the CTX group, treatment with both medium- and high-dose QG (QGM and QGH, respectively), but not low-dose QG (QGL), led to significantly better outcomes ($p < 0.01$ or $p < 0.05$) (Fig. 1). Additionally, the YPF-treated group exceeded the CTX group in terms of index values, but YPF did not affect the hemolysin antibody level.

Regarding the lipopolysaccharide (LPS) stimulation index, all of the model groups had significantly smaller values than the Control group ($p < 0.05$ or $p < 0.01$), and all of the treatment groups had significantly higher values than the CTX group (Fig. 2A). However, the differences with the CTX group were higher in the QGM and QGH groups ($p < 0.01$) than in the QGL and YPF groups ($p < 0.05$).

Immune regulation relies heavily on interleukin (IL)-2 and interferon (IFN)-γ levels. IL-2 has anti-inflammatory properties exerted through inhibition of T-helper 17 cells and increased production of regulatory T cells (TREGs), which are necessary for immunological tolerance and regulation [20], and has a complex role in the immune

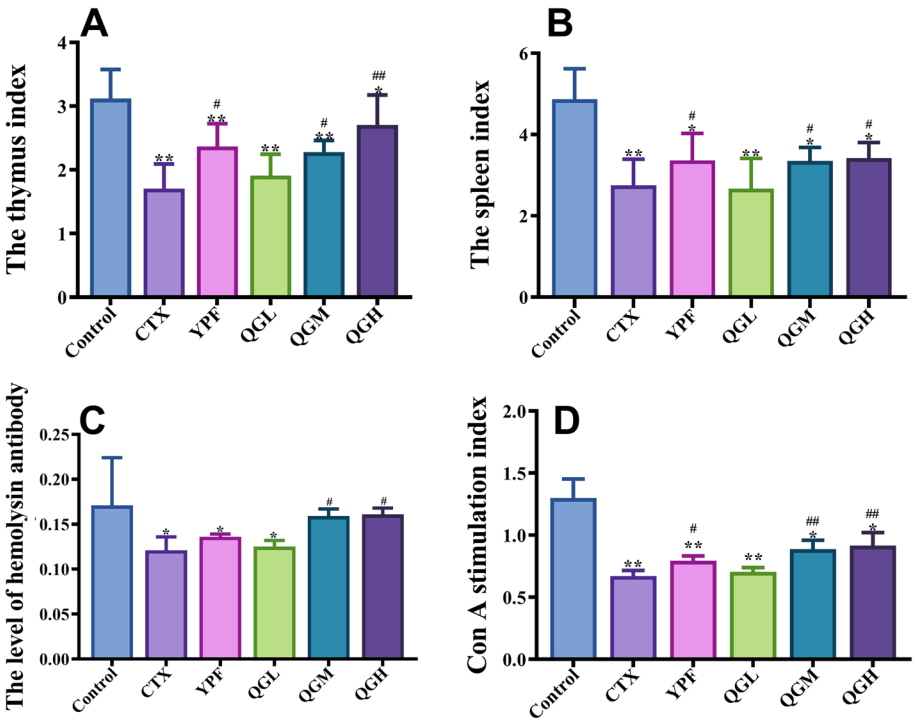

Fig. 1 Effects of Yupingfeng (YPF) and Qi-Gen powder (QG) on immune function in cyclophosphamide (CTX)-induced model mice. **A**–**D** Thymus index (**A**), spleen index (**B**), serum hemolysin antibody levels (**C**), and Con A stimulation index (**D**) in the Control, model (CTX), YPF, and three QG (high-, medium- and low-dose QG: QGH, QGM, and QGL) treatment groups. Data expressed as means ± standard deviation; $^{*}p < 0.05$ and $^{**}p < 0.01$ vs. control group; $^{\#}p < 0.05$ and $^{\#\#}p < 0.01$ vs. CTX group

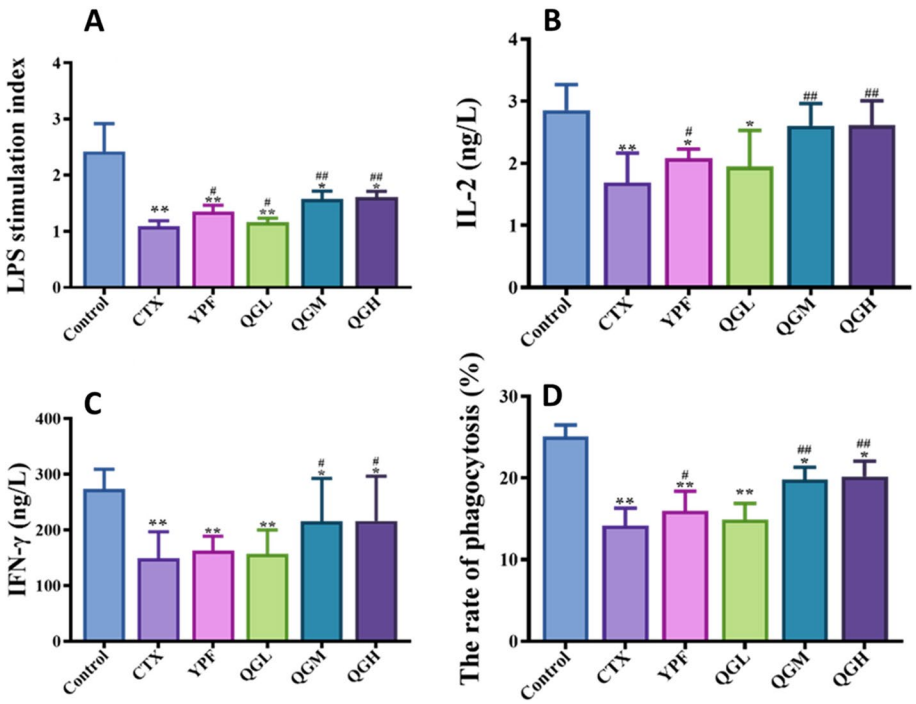

Fig. 2 Effects of YPF and QG on the lipopolysaccharide (LPS) stimulation index and immunoregulatory factors in CTX-induced model mice. **A**–**D** LPS stimulation index (**A**), serum levels of IL-2 (**B**) and interferon (IFN)-γ (**C**), and the rate of phagocytosis (**D**) in the Control, model (CTX), YPF, and three QG (QGH, QGM, and QGL) treatment groups. Data expressed as means ± standard deviation ($n = 10$); $^{*}p < 0.05$ and $^{**}p < 0.01$ vs. Control group; $^{\#}p < 0.05$ and $^{\#\#}p < 0.01$ vs. CTX group

system. IFN-γ exerts anti-inflammatory effects by inhibiting T-helper 17 cells and limiting IL-17 production, regulates immunological responses, and has immunostimulatory effects, helping to maintain immune homeostasis [21, 22]. Regarding the levels of IL-2 (Fig. 2B) and IFN-γ (Fig. 2C) in splenic lymphocyte supernatants, the QGM and QGH groups had significantly better outcomes than the CTX group (both treatment groups $p < 0.01$ for IL-2; $p < 0.05$ for IFN-γ). Treatment with QGL did not have a significant effect on either of these indexes compared to the CTX group, while YPF only had a significant effect on the IL-2 index ($p < 0.05$) (Fig. 2B, C). It is worth noting that the IL-2 index values in both the QGM and QGH groups almost reached those of the Control group.

Macrophage phagocytosis is another indicator of medicinal effects on immune function. In immunosuppressed mice, QGM and QGH treatment led to significant restoration of macrophage phagocytosis, exceeding that in the CTX group (QGM: 19.8% ± 1.5%, $p < 0.01$; QGH: 20.2% ± 1.9%, $p < 0.01$) (Fig. 2D). While treatment with YPF also had a significant effect ($p < 0.05$), treatment with QGL did not.

To distinguish the differences in immune effects between YPF and QG, which also contains YPF, we further examined the results of the above assays in the YPF and QGH groups. The QGH group exceeded the YPF group in thymus index, hemolysin antibody level, Con A and LPS stimulation indexes, IL-2 and IFN-γ content, and phagocytosis rate. These findings suggested that Huangqin and Banlangen, the other main TCM components of QG powder, play important roles in boosting immunity. Taken together, our results indicated that QG enhances immunological function in immunosuppressed mice, particularly at the high and medium doses.

Furthermore, compared with the YPF group, the QGH group mice had significantly improved immune function in terms of thymus index, spleen index, splenic lymphocyte proliferation, and macrophage phagocytosis ($p < 0.05$ or $p < 0.01$). Serum hemolysin antibody levels were significantly higher in both the QGH ($p < 0.01$) and QGM ($p < 0.01$) groups than in the YPF group. QGH treatment also led to greater improvements in immunological organ index, splenic lymphocyte proliferation, IL-2 and IFN-γ concentrations, and macrophage phagocytosis compared to YPF treatment ($p < 0.05$). These findings suggested that QG may provide better immune enhancement under CTX-induced conditions.

Effects of QG on post-vaccination changes in antibody titer, IL-2 and IFN-γ levels, and lymphatic cell proliferation in chickens

To demonstrate the effects of QG treatment on immune function post vaccination, we used an NDV-IV immunization model in chickens (see Tables S1–4 for detailed results). At 7 days post immunization, all immunized groups had significantly higher Newcastle disease antibody titers than the unvaccinated Control group, indicating the effectiveness of NDV-IV vaccination. These antibody titers increased over time in each immunized group, peaking on day 21 or day 28 post vaccine. On all four assessment days, QGM and QGH had considerably stronger impacts on antibody titers than QGL or vaccination alone (Model) ($p < 0.05$), but the two treatment groups (QGM and QGH) did not significantly differ from each other (Fig. 3A).

Similarly, the QGM and QGH groups showed higher levels of IL-2 (Fig. 3C) and IFN-γ (Fig. 3B) compared to the other groups ($p < 0.05$). This difference was especially obvious at 21 days post vaccine. There were no significant differences in the levels of these factors between the QGL and Control group, or between the QGM and QGH groups.

With respect to splenic lymphocyte proliferation, on all four assessment days, all of the vaccinated groups had significantly greater mean values than the Control group ($p < 0.05$), all three QG groups had significantly greater mean values than the Model group ($p < 0.05$), and the QGM and QGH groups had significantly greater mean values than the QGL group ($p < 0.05$). Again, the difference between the QGM and QGH groups was not significant (Fig. 3D).

Effects of QG on post-vaccination immune organ index, bursa index, and body change in weight chickens

Next, the thymus index (Fig. 4A), spleen index (Fig. 4B), and bursa index (Fig. 4C) were compared between groups to evaluate the effects of QG on post-vaccination immune organ responsiveness in chickens (see Tables S5–S8 for detailed results). The values of these three indexes were significantly higher in the QGM and QGH groups than in the other groups ($p < 0.05$), but were not significantly different from each other. Compared with the Model group, the QGL group had a significantly higher thymus index on day 28 post vaccine and significantly higher spleen and bursa indexes on all four assessment days. During the 3rd, 4th, and 5th weeks post immunization ($p < 0.05$), all three QG treatment groups had significantly greater average change of body weight than the Model group (Fig. 4D). These findings demonstrated that administration of QG for 5 days following immunization with NDV-IV significantly increased immunity in chickens.

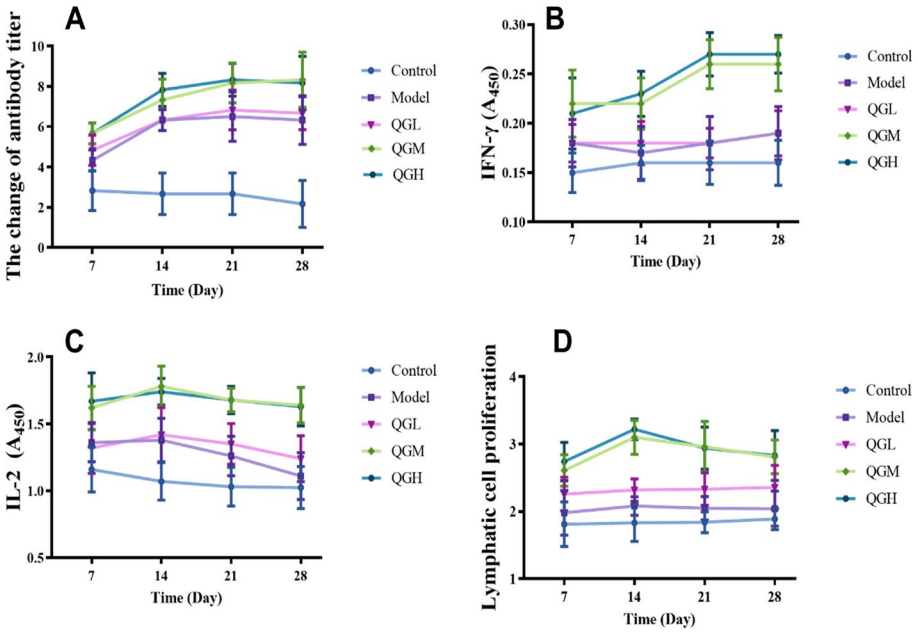

Fig. 3 Effects of QG on Newcastle disease virus (NDV)-IV immunization in chickens. **A**–**D** Changes in antibody titer (**A**), serum levels of IL-2 (**B**) and IFN-γ (**C**), and lymphatic cell proliferation (**D**) in chickens receiving no vaccination (Control), NDV-IV vaccination only (Model), or NDV-IV vaccination followed by 5 days of treatment with low-, medium-, or high-dose QG (QGL, QGM, and QGH, respectively)

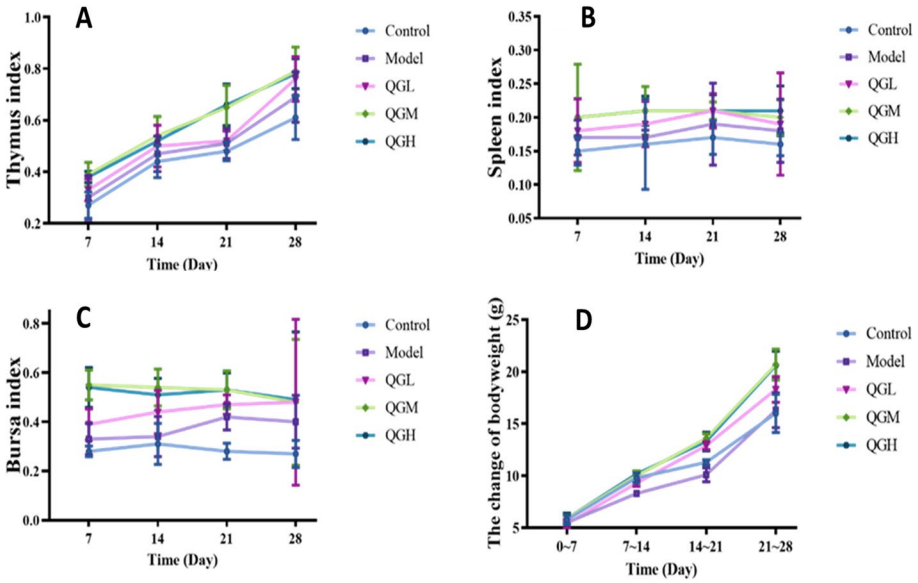

Fig. 4 Effects of QG on post-vaccination immune organ responsiveness in chickens. **A**–**D** Thymus index (**A**), spleen index (**B**), bursa index (**C**), and change of body weight (**D**) in chickens receiving no vaccination (Control), NDV-IV vaccination only (Model), or NDV-IV vaccination followed by 5 days of treatment with low-, medium-, or high-dose QG (QGL, QGM, and QGH, respectively)

Microarray gene expression profiling to verify the therapeutic mechanism of QG

To further investigate the therapeutic mechanism of QG, gene expression profiling was conducted in MCF-7 breast cancer cells treated with 0.075 mg/mL QG for 6 h. We identified 289 DEGs: 118 that were downregulated and 171 that were upregulated (Fig. 5B). Through cluster analysis, we found that the gene expression profiles

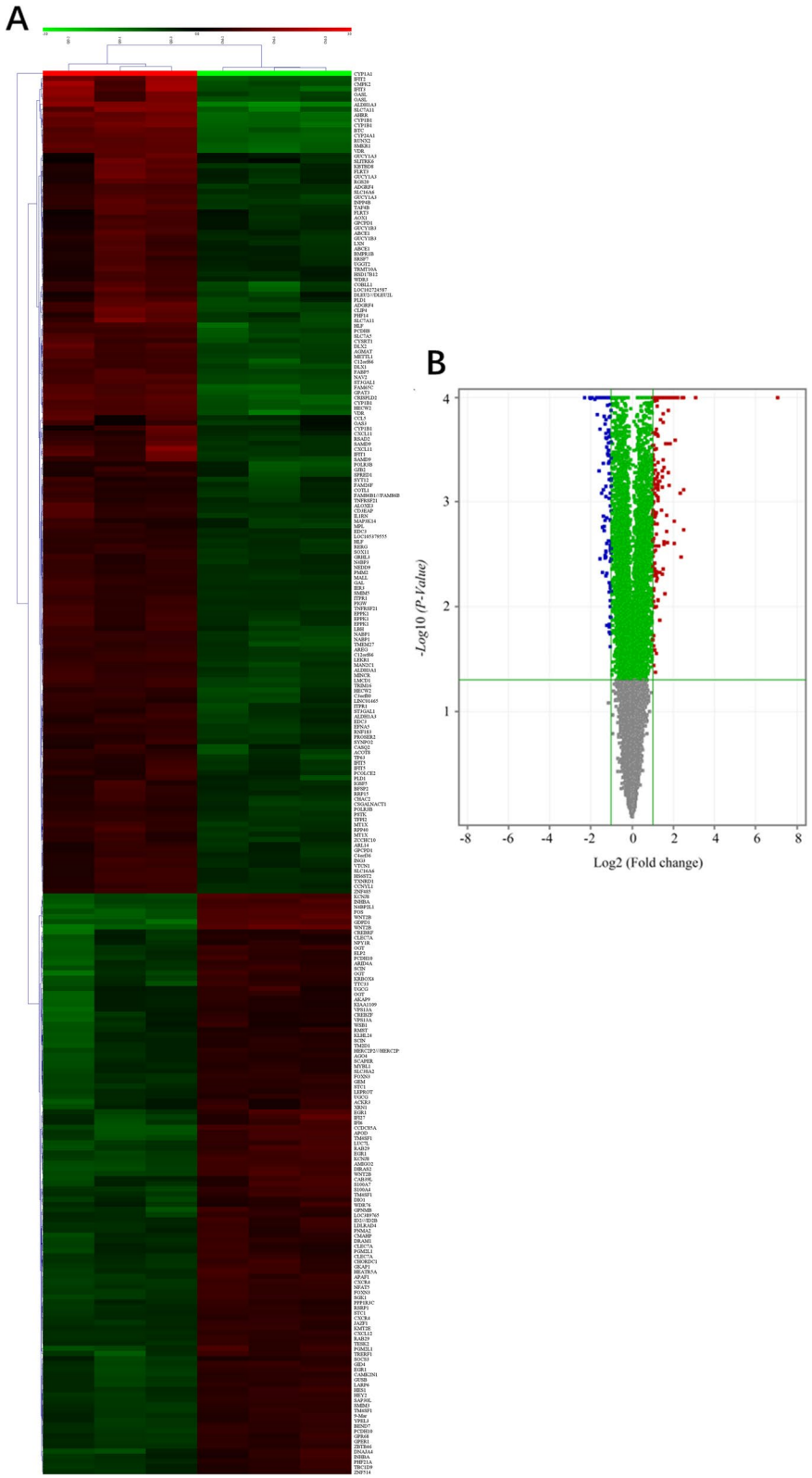

Fig. 5 Microarray gene expression profiling of MCF-7 cells treated with QG. **A**, **B** Heatmap (**A**) and Volcano map (**B**) of differentially expressed genes (DEGs) between treated and untreated cells. Red dots represent significantly upregulated genes, and blue dots represent significantly downregulated genes

of biological replicates in each group were quite similar (Fig. 5A).

The DEGs were used to conduct GO and KEGG analyses to examine the potential effects of QG on immunological function (Table S9). Key GO terms ($p < 0.05$) were identified from the DEGs and filtered for biological importance (Fig. 6A, B). The results showed that the upregulated DEGs were primarily involved in GO biological processes (BP) such as response to virus, type I IFN signaling pathway, defense response to virus, negative regulation of viral genome replication, and nitric oxide (NO)-mediated signal transduction. Their molecular functions (MFs) included oxidoreductase activity, iron ion binding, heparin binding, tRNA binding, and heme binding. The cellular components (CCs) were primarily located in the cytoplasm, which contained 47 DEGs. The downregulated DEGs involved BPs including modulation of sequence-specific DNA binding, transcription factor activity, positive regulation of transcription, and DNA-templated transcription. Negative regulation of transcription from the RNA polymerase II promoter, histone deacetylation, and negative regulation of B-cell differentiation were also enriched. The nucleus, which had 33 DEGs, was the primary site of CCs. The MFs were focused on histone deacetylase activity, transcription factor activity, sequence-specific DNA binding, C-X-C chemokine receptor activity, and sequence-specific DNA binding.

The upregulated DEGs were found to be involved in metabolic pathways, cytochrome P450-mediated xenobiotic metabolism, chemical carcinogenesis, tyrosine metabolism, tryptophan metabolism, and herpes simplex infection, whereas the downregulated DEGs were not significantly involved in any pathways (Fig. 6A, B).

The cMap analysis (Table S10) was extremely helpful in drug prediction and drug target selection. The DEGs in QG-treated cells indicated that effect of QG act similarly to many well-known small molecules. According to the findings, 30 small molecules had opposite effects to QG and 27 small molecules had QG-like effects. Glycogen synthase kinase inhibitors, RAF inhibitors, and protein synthesis inhibitors all have comparable mechanisms of action, whereas PI3K inhibitors have opposite effects.

Discussion

With the advancement in contemporary TCM pharmacology, it is now possible to analyze TCMs using precise models that accurately assess their efficacies and comprehend their mechanisms from the perspective of evidence-based medicine. In this study, we assessed the immune-enhancing efficacy of a new TCM formula, QG,

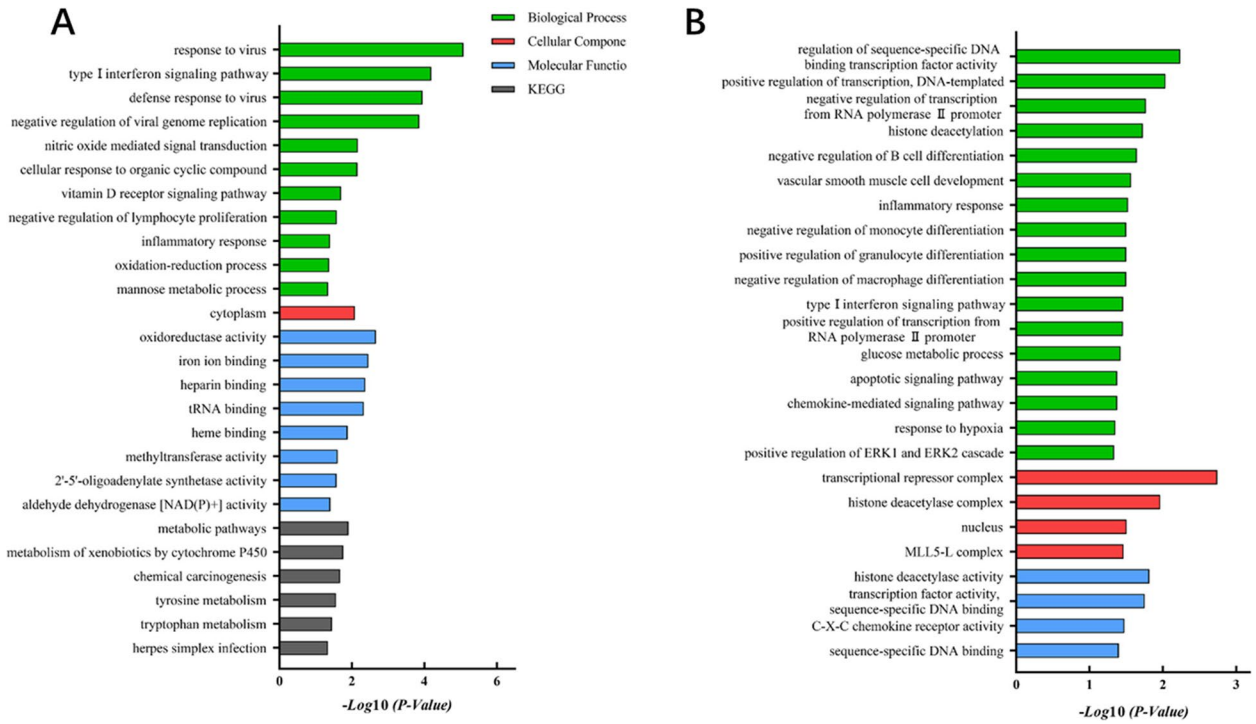

Fig. 6 GO annotation and KEGG pathway analyses of DEGs in MCF-7 cells treated with QG. **A**, **B** Upregulated DEGs (**A**) and downregulated DEGs (**B**) ($p < 0.05$)

and explored potential therapeutic mechanisms. QG was created by combining YPF, a traditional remedy that aims to boost "Qi", strengthen the body surface resistance, and provide physiological immune-enhancing effects, with two other traditional Chinese remedies, Huangqin and Banlangen. The term "Qi" in TCM refers to an element that energizes and permeates the entire human body.

Using immunosuppressed mice, we found that the additions of Huangqin and Banlangen boosted the ability of the formula to regulate immunological responses. Our investigation revealed that mice treated with QG (medium or high dose) showed significant improvements in immune organ index, serum hemolysin antibody levels, Con A and LPS stimulation index, IL-2 and IFN-γ content, and rate of phagocytosis compared to those administered YPF (Figs. 1 and 2). YPF has been used to treat inflammatory diseases and served as a positive control in the present study. YPF reportedly improves the body weight loss caused by dexamethasone, reduces thymus and spleen coefficients, and recovers lymphocyte function [8]. Additionally, YPF exhibited an immunoregulatory effect in a rat model of chronic bronchitis [12]. These findings indicate that YPF regulates cellular and nonspecific immunity, acts as an immunomodulator, and improves immune function in immunocompromised animals. In our CTX-induced mice, the effects of QG exceeded those of YPF in immunoregulation, suggesting that the addition of Banlangen and Huangqin enhance the efficacy of the original formula. Indeed, Banlangen and Huangqin have previously been found to have immune-regulating properties [23, 24].

Treatment of immunosuppressed mice with a medium or high dose of QG also had restorative effects on the immune system of CTX model mice. These findings included increased growth of splenic lymphocytes, a potential indicator of mouse immunity, and a better response to Con A, an inhibitor of splenic lymphocyte proliferation, in QG-treated CTX mice.

QG administration improved body weight gain in NDV-IV immunized chickens, possibly through upregulated mRNA expression of *SGLT1*, *GLUT2*, and *GLUT5* in the intestine [25], or growth promotion by baicalin, the main active component of Huangqin [26]. Further research is needed to investigate these potential QG mechanisms. Lymphocyte proliferation reflects the overall health of the immune system [27]. T cells and B cells bear surface antigen recognition receptors and mitogen receptors that stimulate lymphocyte clones to proliferate in response to specific antigens. Con A selectively stimulates T-cell proliferation [28], while LPS promotes B-cell proliferation [29]. LPS was shown to inhibit splenic lymphocyte proliferation in this study (Fig. 2A). QG restored T- and B-lymphocyte proliferation to some extent, regulating humoral and innate immunity. This finding was consistent with the identification of treatment-related DEGs such as GO:0009615 (response to virus) and GO:0060337 (type I IFN signaling pathway).

This study also employed gene chip technology to investigate the putative role of QG in immunological modulation. Gene expression profiling revealed that several immune-related genes were strongly regulated following QG therapy. The type I IFN signaling pathway was shown to be the most significantly regulated pathway in GO and KEGG pathway analyses. According to the findings of this study, QG treatment significantly increased the antiviral action of IFNs. Infected cells release IFN, which is regulated by the induction of antiviral proteins expressed by members of the IFN-induced tetrapeptide repeat family (IFIT), including *IFIT1*, *IFIT2*, *IFIT3*, and *IFIT5* [30]. Baicalein, Huangqin, and Banlangen have been shown to promote immune function [26, 31], while *Radix Isatidis* polysaccharides [14, 32] are thought to increase IFN-γ production. Additionally, astragaloside III, the main active components of Huangqin and Baizhu [33], and total polysaccharides from *Atractylodis macrocephalae* [34, 35] all promote the production of IFNs including IFN-γ.

The genes *OAS3* and *OASL*, which activate RNaseL, were also among the DEGs [36]. GO:0009615 (reaction to virus), GO:0060337 (type I IFN signaling pathway), GO:0051607 (defense response to virus), and GO:0045071 (negative regulation of viral genome replication) were significantly upregulated and primarily related to innate immune (Table S9). Additionally, *CYP1A1* and *CYP24A1*, which encode members of the cytochrome P450 superfamily of enzymes, are enriched in hsa01100 (Metabolic pathways), hsa00980 (Metabolism of xenobiotics by cytochrome P450), GO:0009615 (response to virus), and GO:0070561 (vitamin D receptor signaling pathway). These pathways and BPs catalyze many reactions involved in drug metabolism and the synthesis of cholesterol, steroids, and other lipids [37]. *CYP24A1*-encoded enzymes regulate vitamin D3 levels in calcium homeostasis and the vitamin D endocrine system [38], thus affecting innate and adaptive immunity by altering vitamin D and participating in calcium and phosphorus metabolism [39].

The cMap database was used to examine the gene chip results for potential identification of small-molecule medications that resemble QG. The greater the cMap score of a small compound, the more likely its drug action is equivalent to that of QG. As shown in Table S10, the glycogen synthase kinase (GSK)-3-inhibitor IX had the highest cMap score of 99.93, indicating that it was a GSK inhibitor, lipoxygenase inhibitor, or protein kinase C inhibitor. The presence of GSK-3 inhibitors increase IL-2 secretion [40, 41], and GSK-3 inhibitor IX decreases viral gene transcription of the

white spot syndrome virus by inhibiting and inactivating GSK-3 [42]. Using the TCMSP platform, we identified active components targeting GSK-3β in Huangqi, Banlangen, Fangfeng, and Huangqin. In this study, 12 of the 30 small molecules identified were found to be phosphatidylinostitol-3-kinase (PI3K) inhibitors with opposite effects to QG. Upregulation of IL-2 expression may be related to activation of the PI3K/AKT signaling pathway [43, 44]. These results were consistent with those in the animal studies and cMap analysis, leading us to hypothesize that the PI3K/Akt/GSK-3 signaling pathway is required for QG-mediated immune system modulation. In this study, bioinformatics was mainly used to analyze the possible therapeutic mechanisms of QG, and quantitative real-time PCR was needed to verify the analysis results of gene chips in the future.

The experiment designed to determine whether QG could boost the effectiveness of the NDV vaccine in chickens indicated that, regardless of the dose, each QG treatment group exhibited rapid increases in antiviral antibody titers, as well as the levels of IFN-γ and IL-2, in the early post-immunization period. The immune organ indexes and peripheral blood lymphocyte proliferation activity were also significantly increased, especially with medium- or high-dose QG. These findings suggested that QG boosts chicken immunity through an immunological response to the vaccine.

Conclusions

QG altered both non-specific cellular immunity and specific humoral immunity, and had a greater pharmacological impact than YPF. QG also enhanced the chicken immune responses to NDV vaccination. GO and KEGG analysis of DEGs revealed that QG largely influenced the response to virus, type I IFN signaling pathway, defensive response to virus, and negative control of viral genome replication. The therapeutic mechanism was further studied using cMap and TCMSP, which substantiated our hypothesis regarding the connection between QG-mediated immune regulation and the PI3K/Akt/GSK-3 pathway. Further mechanistic investigations are needed to validate this hypothesis.

Materials and methods

Preparation of QG powder

QG powder was produced by combining YPF, a classical Chinese herbal formula, with two herbal remedies, Banlangen and Huangqin. The key ingredients of the YPF formula (known as Gyokuheifu-san in Japanese and Jade Windscreen powder in English) are Huangqi (Astragali Radix, *Astragalus propinquus* Schischkin, Leguminosae), Baizhu (Atractylodis Macrocephalae Rhizoma, *Atractylodes macrocephala* Koidzumi, Compositae), and Fangfeng (Saposhnikoviae Radix, *Saposhnikoviae divaricata* [Turcz.] Schischk., Umbelliferae). The QG powder evaluated in this study comprised Huangqi, Banlangen, Fangfeng, stir-fried Baizhu, and Huangqin, blended in a 12:4:4:4:3 ratio. After extraction, the powder was processed into 1000 g; for every 1 g of QG, 1.35 g of crude drug was required. The five Chinese herbs in QG were certified using the authentication processes used by the Chinese Pharmacopoeia (see Figures S1–S3 for the techniques used).

Chinese herbs, chemicals, and reagents

See Supplementary Materials for details.

Animals

Both sexes Kunming (KM) mice (license no. SCXK [LU] 20,140,001) weighing 18–22 g were purchased from Qingdao Experimental Animals and Animal Experimental Center. The Beijing Keao Xieli Feed Co., Ltd. provided the mouse maintenance feed. The mice were pre-fed for 1 week before the trial began. Male Xinsu broiler chickens (age: 1 day) were purchased from the Chinese Academy of Agricultural Sciences Institute of Poultry. The chickens were raised normally and allowed to eat and drink freely with regular feed and water (without any drugs) until 7 days of age. Their beaks were removed at 5 days of age. China Agricultural University Laboratory Animal Welfare and Animal Experimental Ethical Committee approved the study and provided the guidelines for studies involving animals.

QG treatment and immunologic function assessment in immunosuppressed mice

The experiments included a total of 240 KM mice randomly divided into six groups: Control, CTX (CTX-induced model only), YPF (CTX-induced and treated with YPF, 1.41 mL/kg body weight (b.w.)), QGH (CTX-induced and treated with high-dose QG, 2.82 g/kg b.w.), QGM (CTX-induced and treated with medium-dose QG, 1.41 g/kg b.w.), and QGL (CTX-induced and treated with low-dose QG, 0.71 g/kg b.w.). The dose was calculated using the suggested dose in the QG guidelines (announcement No. 187 of the Ministry of Agriculture and Rural Affairs of China in 2019), the medium dose was equivalent to the suggested dose for QG in clinical practice. For 5 consecutive days (days 1–5), mice in the Control and CTX groups were given 0.23 mL 0.9% saline, while the four treatment groups received the appropriate dosage of YPF, QGH, QGM, or QGL. Except for the Control group, all other groups received intraperitoneal injections of 80 mg/kg CTX once a day for 3 days, starting on day 3 of the experiment.

At the end of the treatment (day 5), the thymus and spleen indexes, serum hemolysin antibody levels, phagocytic function of mouse peritoneal macrophages, and proliferation of splenic lymphocytes were determined in each mouse (see Supplementary Materials for details).

QG treatment and assessment of NDV-immunized chickens

A total of 180 chickens (age: 7 days) were randomly divided into five groups: Control, Model (vaccination only), QGH (vaccination with high-dose QG, 4.0 g/L), QGM (vaccination with medium-dose QG, 2.0 g/L; the suggested dosage based on QG instructions in Announcement No. 187 of the Ministry of Agriculture and Rural Affairs of China in 2019), and QGL (vaccination with low-dose QG, 1.0 g/L). All vaccination group chickens were administered 100 μL NDV-IV via intratracheal and nasal routes. Except for the Control group (saline alone), all other groups were being administered the prescribed medicine for 5 days after 12 h of immunization.

To obtain serum, blood was collected from the jugular veins of 10 chickens randomly selected from each group on days 7, 14, 21, and 28 post immunization. The hemagglutination inhibition method was used to determine antibody titers against NDV. The measured agglutination value for the NDV-LaSota virus is $1:2^8$. The antibody titer, defined as log 2, is the highest serum dilution with complete agglutination inhibition. Serum samples were also tested for IL-2 and IFN-γ levels using enzyme-linked immunosorbent assay kits. Optical density values were measured at 450 nm in accordance with the kit instructions.

Six chickens were chosen at random from each group on days 7, 14, 21, and 28 post immunization, weighed them, and blood was drawn from the jugular vein and 1.5 mL was immediately transferred to a sterile container. The 3-(4,5-dimethylthiazol-2-yl)-2,5-diphenyltetrazolium bromide (MTT) method was used to distinguish lymphocytes in the peripheral blood. In addition, the thymus, spleen and bursae of these chickens were collected and the organ index calculated.

Following immunization, feed consumption in all chickens in each group was measured on days 0–7, 7–14, 14–21, and 21–28 post immunization. The daily increase in weight (g/day/feather) was determined using the following formula:

$$\textit{Daily weight gain} = \frac{\textbf{average final weight} - \textbf{average starting weight}}{\textbf{feeding days}}$$

Cell culture

The breast cancer cell line MCF-7 was maintained in Dulbecco's modified Eagle medium supplemented with 10% fetal bovine serum, 100 U/mL penicillin, and 100 g/mL streptomycin, and incubated at 37 °C in a water-saturated environment with 5% CO_2.

Gene expression profiling analysis

MCF-7 cells were treated with QG (0.075 mg/mL) for 6 h ($n=3$); three repeat samples were also collected for the untreated MCF-7 cells. Total RNA from MCF-7 cells was extracted using TRIzol reagent (Thermo Fisher Scientific, Carlsbad, CA, USA) in accordance with the manufacturer's instructions.

Affymetrix Human Genome U133 Plus 2.0 arrays (Affymetrix, Santa Clara, CA, USA) were hybridized with total RNA that had been reverse transcribed to cDNA. An Affymetrix GeneChip Command Console (version 4.0) was used to evaluate array images and obtain raw data. Genespring software with the RMA algorithm (version 13.1, Agilent Technologies) was used to normalize the raw data. DEGs were identified on the basis of t-tests (criteria: $p < 0.05$; fold change value = 2.0 up or down) and visualized using a volcano chart. Hierarchical clustering was used to depict the expression patterns of various DEGs. The Database for Annotation, Visualization and Integrated Discovery (DAVID, version 6.8; https://david.ncifcrf.gov/) was used for GO annotation and KEGG analyses to determine the functions of these DEGs.

Statistical analysis

All data are expressed as means ± standard deviation. Antibody titers, lymphocyte proliferation, and growth performance were compared between groups using one-way analysis of variance and Duncan's multiple comparisons test. Chi-square tests were used to compare the rates of incidence, mortality, and protection between groups (IBM SPSS statistical software, version 20.0). A $p < 0.05$ was defined as a statistically significant difference between groups.

Supplementary Information

The online version contains supplementary material available at https://doi.org/10.1186/s44280-024-00055-x.

Supplementary Material 1

Acknowledgements
This study was supported by the Beijing Municipal Science and Technology Commission (grant number: Z191100001619001), and Key project at central government level: The ability to establish sustainable use of valuable Chinese medicine resources (grant number: 2060302).

Authors' contributions
X.G. wrote the paper. X.G., S.W. and D.M. conducted data analysis. P.W., F.Y., X.X. and T.H. completed the experiments. H.X. and Z.H. designed this study. All authors contributed to the article and approved the submitted version.

Funding
Beijing Municipal Science and Technology Commission (grant number: Z191100001619001), and Key project at central government level: The ability to establish sustainable use of valuable Chinese medicine resources (grant number: 2060302).

Availability of data and materials
The data are available from the corresponding author on reasonable request.

Declarations

Ethics approval and consent to participate
Ethical approval was reviewed and given by China Agricultural University Laboratory Animal Welfare and Animal Experimental Ethical Committee (AW02604202-2–1). All the animal experimental procedures strictly conducted by Chinese laws and guidelines.

Consent for publication
Not applicable.

Competing interests
No potential conflict of interest was reported by the authors.

Received: 4 October 2023 Revised: 23 June 2024 Accepted: 1 July 2024
Published online: 30 August 2024

References

1. Rothan HA, Byrareddy SN. The epidemiology and pathogenesis of coronavirus disease COVID-19 outbreak. J Autoimmun. 2020;109:102433.
2. Zumla A, Chan JF, Azhar EI, Hui DS, Yuen KY. Coronaviruses - drug discovery and therapeutic options. Nat Rev Drug Discov. 2016;15:327–47.
3. Lycett SJ, Duchatel F, Digard P. A brief history of bird flu. Philos Trans R Soc Lond B Biol Sci. 2019;374:20180257.
4. Blome S, Staubach C, Henke J, Carlson J, Beer M. Classical swine fever-an updated review. Viruses. 2017;9:86.
5. Bonam SR, Partidos CD, Halmuthur SKM, Muller S. An overview of novel adjuvants designed for improving vaccine efficacy. Trends Pharmacol Sci. 2017;38:771–93.
6. Boopathy AV, Mandal A, Kulp DW, Menis S, Bennett NR, Watkins HC, et al. Enhancing humoral immunity via sustained-release implantable microneedle patch vaccination. Proc Natl Acad Sci U S A. 2019;116:16473–8.
7. Ma HD, Deng YR, Tian Z, Lian ZX. Traditional Chinese medicine and immune regulation. Clin Rev Allergy Immunol. 2013;44:229–41.
8. Li Y, Zheng B, Tian H, Xu X, Sun Y, Mei Q, et al. Yupingfeng powder relieves the immune suppression induced by dexamethasone in mice. J Ethnopharmacol. 2017;200:117–23.
9. Zhang L, Wei W. Anti-inflammatory and immunoregulatory effects of paeoniflorin and total glucosides of paeony. Pharmacol Ther. 2020;207:107452.
10. Su X, Pei Z, Hu S. Ginsenoside Re as an adjuvant to enhance the immune response to the inactivated rabies virus vaccine in mice. Int Immunopharmacol. 2014;20(2):283–9.
11. Wang M, Mao D, Li H. Chinese medicine Jiedu Huayu granules reduce liver injury in rats by regulating T-cell immunity. Evid Based Complement Alternat Med. 2019;2019:1873541.
12. Song J, Li J, Zheng SR, Jin Y, Huang Y. Anti-inflammatory and immunoregulatory effects of Yupingfeng powder on chronic bronchitis rats. Chin J Integr Med. 2013;19:353–9.
13. Yang J, Yang X, Li M. Baicalin, a natural compound, promotes regulatory T cell differentiation. BMC Complement Altern Med. 2012;12:64.
14. Zhao YL, Wang JB, Shan LM, Jin C, Ma L, Xiao XH. Effect of Radix isatidis polysaccharides on immunological function and expression of immune related cytokines in mice. Chin J Integr Med. 2008;14:207–11.
15. Wen Z, Wang Z, Wang S, Ravula R, Yang L, Xu J, et al. Discovery of molecular mechanisms of traditional Chinese medicinal formula Si-Wu-Tang using gene expression microarray and connectivity map. PLoS One. 2011;6:e18278.
16. Nagrath S, Sequist LV, Maheswaran S, Bell DW, Irimia D, Ulkus L, et al. Isolation of rare circulating tumour cells in cancer patients by microchip technology. Nature. 2007;450:1235–9.
17. Schena M, Heller RA, Theriault TP, Konrad K, Lachenmeier E, Davis RW. Microarrays biotechnology's discovery platform for functional genomics. Trends Biotechnol. 1998;16:301–6.
18. Lamb J, Crawford ED, Peck D, Modell JW, Blat IC, Wrobel MJ, et al. The Connectivity Map: using gene-expression signatures to connect small molecules, genes, and disease. Science. 2006;313:1929–35.
19. Ru J, Li P, Wang J, Zhou W, Li B, Huang C, et al. TCMSP: a database of systems pharmacology for drug discovery from herbal medicines. J Cheminform. 2014;6:13.
20. Bachmann MF, Oxenius A. Interleukin 2: from immunostimulation to immunoregulation and back again. EMBO Rep. 2007;8(12):1142–8.
21. Berktas M, Guducuoglu H, Bozkurt H, Onbasi KT, Kurtoglu MG, Andic S. Change in serum concentrations of interleukin-2 and interferon-gamma during treatment of tuberculosis. J Int Med Res. 2004;32(3):324–30.
22. Safont G, Villar-Hernández R, Smalchuk D, Stojanovic Z, Marín A, Lacoma A, et al. Measurement of IFN-γ and IL-2 for the assessment of the cellular immunity against SARS-CoV-2. Sci Rep. 2024;14(1):1137.
23. Shin EK, Kim DH, Lim H, Shin HK, Kim JK. The anti-inflammatory effects of a methanolic extract from *Radix Isatidis* in murine macrophages and mice. Inflammation. 2010;33:110–8.
24. Li H, Wang P, Huang F, Jin J, Wu H, Zhang B, et al. Astragaloside IV protects blood-brain barrier integrity from LPS-induced disruption via activating Nrf2 antioxidant signaling pathway in mice. Toxicol Appl Pharmacol. 2018;340:58–66.
25. Yin F, Lan R, Wu Z, Wang Z, Wu H, Li Z, et al. Yupingfeng polysaccharides enhances growth performance in Qingyuan partridge chicken by up-regulating the mRNA expression of SGLT1, GLUT2 and GLUT5. Vet Med Sci. 2019;5:451–61.
26. Zhou Y, Mao S, Zhou M. Effect of the flavonoid baicalein as a feed additive on the growth performance, immunity, and antioxidant capacity of broiler chickens. Poult Sci. 2019;98:2790–9.
27. Sun H, Sun C, Xiao W, Sun R. Tissue-resident lymphocytes: from adaptive to innate immunity. Cell Mol Immunol. 2019;16(3):205–15.
28. Ando Y, Yasuoka C, Mishima T, Ikematsu T, Uede T, Matsunaga T, et al. Concanavalin A-mediated T cell proliferation is regulated by herpes virus entry mediator costimulatory molecule. In Vitro Cell Dev Biol Anim. 2014;50(4):313–20.
29. Xu H, Liew LN, Kuo IC, Huang CH, Goh DL, Chua KY. The modulatory effects of lipopolysaccharide-stimulated B cells on differential T-cell polarization. Immunology. 2008;125(2):218–28.
30. Zhou X, Michal JJ, Zhang L, Ding B, Lunney JK, Liu B, et al. Interferon induced IFIT family genes in host antiviral defense. Int J Biol Sci. 2013;9:200–8.
31. Orzechowska B, Chaber R, Wiśniewska A, Pajtasz-Piasecka E, Jatczak B, Siemieniec I, et al. Baicalin from the extract of Scutellaria baicalensis affects the innate immunity and apoptosis in leukocytes of children with acute lymphocytic leukemia. Int Immunopharmacol. 2014;23:558–67.
32. Han J, Jiang X, Zhang L. Optimisation of extraction conditions for polysaccharides from the roots of *Isatis tinctoria* L. by response surface

methodology and their *in vitro* free radicals scavenging activities and effects on IL-4 and IFN-γ mRNA expression in chicken lymphocytes. Carbohydr Polym. 2011;86:1320–6.
33. Chen X, Chen X, Gao J, Yang H, Duan Y, Feng Y, et al. Astragaloside III enhances anti-tumor response of NK cells by elevating NKG2D and IFN-γ. Front Pharmacol. 2019;10:898.
34. Xu W, Fang S, Cui X, Guan R, Wang Y, Shi F, et al. Signaling pathway underlying splenocytes activation by polysaccharides from *Atractylodis macrocephalae Koidz*. Mol Immunol. 2019;111:19–26.
35. Xu W, Fang S, Wang Y, Chi X, Ma X, Zhang T, et al. Receptor and signaling pathway involved in bovine lymphocyte activation by *Atractylodis macrocephalae* polysaccharides. Carbohydr Polym. 2020;234:115906.
36. Samuel CE. Antiviral actions of interferons. Clin Microbiol Rev. 2001;14:778–809.
37. Zanger UM, Schwab M. Cytochrome P450 enzymes in drug metabolism: regulation of gene expression, enzyme activities, and impact of genetic variation. Pharmacol Ther. 2013;138:103–41.
38. Prosser DE, Jones G. Enzymes involved in the activation and inactivation of vitamin D. Trends Biochem Sci. 2004;29:664–73.
39. Di Rosa M, Malaguarnera M, Nicoletti F, Malaguarnera L. Vitamin D3: a helpful immuno-modulator. Immunology. 2011;134:123–39.
40. Ohteki T, Parsons M, Zakarian A, Jones RG, Nguyen LT, Woodgett JR, et al. Negative regulation of T cell proliferation and interleukin 2 production by the serine threonine kinase Gsk-3. J Exp Med. 2000;192:99–104.
41. Song YC, Tang SJ, Lee TP, Hung WC, Lin SC, Tsai CY, et al. Reversing interleukin-2 inhibition mediated by anti-double-stranded DNA autoantibody ameliorates glomerulonephritis in MRL-lpr/lpr mice. Arthritis Rheum. 2010;62:2401–11.
42. Sun J, Ruan L, Zhou C, Shi H, Xu X. Characterization and function of a β-catenin homolog from *Litopenaeus vannamei* in WSSV infection. Dev Comp Immunol. 2017;76:412–9.
43. Pellom ST Jr, Dudimah DF, Thounaojam MC, Uzhachenko RV, Singhal A, Richmond A, et al. Bortezomib augments lymphocyte stimulatory cytokine signaling in the tumor microenvironment to sustain $CD8^{+}$T cell antitumor function. Oncotarget. 2017;8:8604–21.
44. Zheng N, Sun L, Pang G, Zha X, Niu W, Tan L, et al. *Chlamydia muridarum* infection induces $CD4^{+}$ T cells apoptosis via PI3K/AKT signal pathway. Pathog Dis. 2019;77:ftz029.

Publisher's Note